FUZZY MAPPING OF DYNAMIC FUNCTIONS TO CONTROL ROBOT MANIPULATORS IN THE OPERATIONAL SPACE

Douglas Wildgrube Bertol, dwbertol@das.ufsc.br
Victor Barasuol, victor@das.ufsc.br
Edson Roberto De Pieri, edson@das.ufsc.br
Universidade Federal de Santa Catarina - UFSC - BOX 88040-900 - Florianópolis - SC

Nardênio Almeida Martins, nardenio@din.uem.br
Universidade Estadual de Maringá - UEM - BOX 87020-900 - Maringá - PR

Abstract. *In this paper a control strategy composed by fuzzy mapped nonlinear terms based on the robot dynamic model is proposed. The proposed controller is evaluate on a research robot manipulator performing a task in the operational space. The tests attempt to achieve fast motion with reasonable accuracy associated with lower computational load compared to the conventional approach. A stability analysis to conclude about the mapping error influence and to obtain precondition criteria to the gains adjustment face to a trajectory tracking problem is presented. Experimental tests are conducted on a robot manipulator with SCARA configuration, to demonstrate the feasibility of this strategy.*

Keywords: *robot manipulators, nonlinear control, operational space control, fuzzy mapping*

1. INTRODUCTION

When robot manipulators are requested to perform agile motion, conventional strategies based on PD (proportional-derivative) action may become inaccurate due to inherent nonlinear dynamics existing in the real mechanisms. Facing these problems, the control action must be enhanced in such a way to incorporate some model features.

Other difficulties arises when the characteristics of the model comprise the control action and the tasks are performed in the operational space and controlled in the joint space. This control action becomes even more complex, since the mathematical transformations require a substantial number of matrix operations, resulting in an excessive computational load (considering the average capacity of processing cores embedded in robot manipulators) and the magnitudes of the partial error become more expressive due to parametric uncertainties.

A control methodology has been used to circumvent those inconveniences by using kinematics transformations, leading the control paradigm to the operational space, relating the joint torques to forces in the operational space by means of the Jacobian matrix (Sciavicco and Siciliano, 2000). To illustrate, in Fig. 1 are depicted the control structure in the joint space (left) and in the operational space (right), where $\boldsymbol{P}_\mathrm{d} = [\boldsymbol{p}_\mathrm{d}\ \dot{\boldsymbol{p}}_\mathrm{d}\ \ddot{\boldsymbol{p}}_\mathrm{d}]$ is the matrix of desired trajectory in the operational space, $\boldsymbol{P} = [\boldsymbol{p}\ \dot{\boldsymbol{p}}\ \ddot{\boldsymbol{p}}]$ is the matrix of posture in the operational space, $\boldsymbol{Q}_\mathrm{d} = [\boldsymbol{q}_\mathrm{d}\ \dot{\boldsymbol{q}}_\mathrm{d}\ \ddot{\boldsymbol{q}}_\mathrm{d}]$ is the matrix of desired trajectory in the joint space, $\boldsymbol{Q} = [\boldsymbol{q}\ \dot{\boldsymbol{q}}\ \ddot{\boldsymbol{q}}]$ is the matrix of posture in the joint space and $\boldsymbol{\tau} = [\tau_1\ \tau_2]^\mathrm{T}$ is the vector of joint control torques.

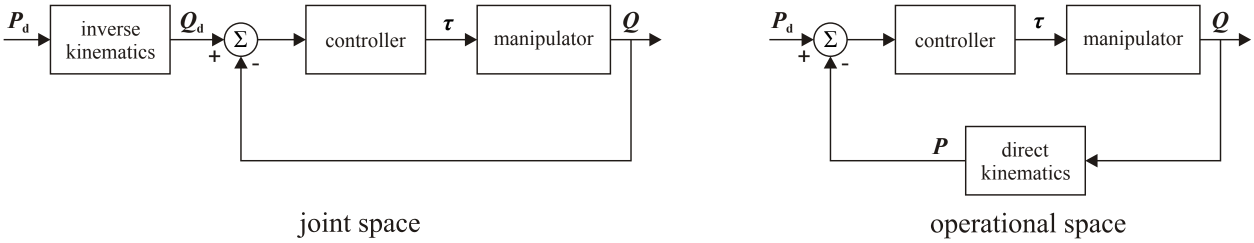

Figure 1. Control structures

Fuzzy sets and systems have passed by a substantial development since it was introduced by Zadeh (1973). The most used inference process was proposed by Mamdani (1974). However, in this work we used the Sugeno inference process (Takagi and Sugeno, 1985), also known as Takagi-Sugeno-Kang or T-S fuzzy.

Among the features of fuzzy systems, there are two of them that justify its use in this study: the possibility of identifying only systems using sets of input-output pairs (Zhang and Liu, 2006) and the possibility to reduce the order of the system model with consequent reduction of computational load (Tanaka and Wang, 2002).

To treat the operational space control problem with agile motion and low computational load, a control action with addition of model-based nonlinear terms is proposed. However, these terms are mapped by a fuzzy inference system. This fuzzy mapping provides the capability of reducing the amount of mathematical operations of the control law, decreasing the computational load.

This paper is organized as follow: in Section 2 are described the the mathematical model of the robot manipulator and its relations and transformations necessary to perform the operational space control. In Section 3 section are presented the proposed control action, the stability analysis of the system is treated in Section 4. In the Section 5 are reported the details of the mapping process. Finally, the experiments results and the conclusions are presented in Sections 6 and 7, respectively.

2. MATHEMATICAL MODEL OF THE ROBOT MANIPULADOR

For the experiments it was used a robot manipulator, Fig. 2, with a SCARA (Selective Compliant Assembly Robot Arm) configuration. This robot, that was made in Zurich by *Eidgenössische Technische Hochschule* (ETH), is used only for academic research in the *Laboratório de Controle e Automação* (LCA) of the *Departamento de Automação e Sistemas* (DAS) in the *Universidade Federal de Santa Catarina* (UFSC).

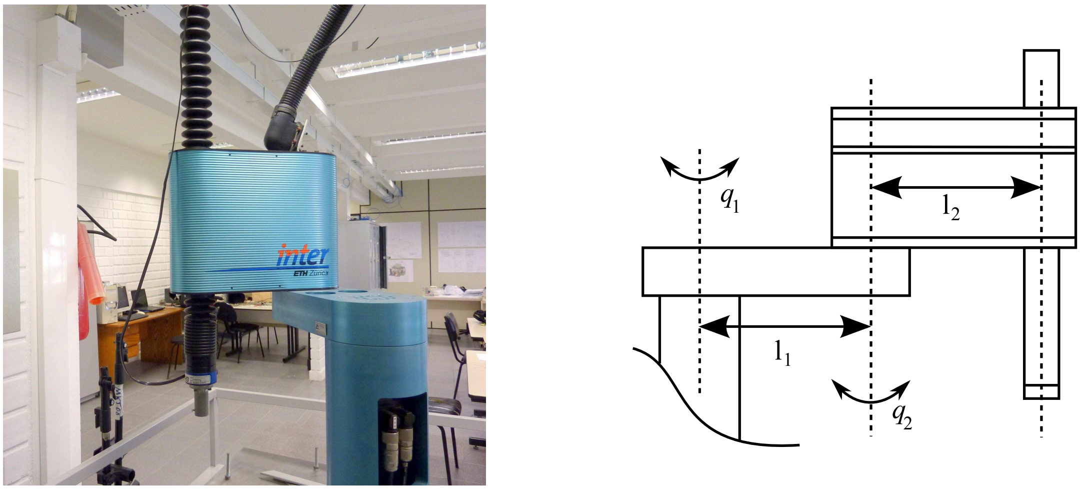

Figure 2. SCARA robot

The robot manipulator dynamics can be written according to the following mathematical model (Siciliano and Khatib, 2008):

$$\boldsymbol{B}(\boldsymbol{q})\ddot{\boldsymbol{q}} + \boldsymbol{C}(\boldsymbol{q},\dot{\boldsymbol{q}})\dot{\boldsymbol{q}} + \mathbf{F}\dot{\boldsymbol{q}} + \boldsymbol{g}(\boldsymbol{q}) = \boldsymbol{\tau}. \tag{1}$$

Equation (1) describes the robot manipulator dynamics in the joint space, where: $\boldsymbol{B}(\boldsymbol{q})$ is the inertia matrix, $\boldsymbol{C}(\boldsymbol{q},\dot{\boldsymbol{q}})$ is the Coriolis and centrifugal forces matrix, $\mathbf{F}$ is the friction forces matrix, $\boldsymbol{g}(\boldsymbol{q})$ is the gravitational forces vector and $\boldsymbol{\tau}$ is the joint torques vector.

By using the relational property $\dot{\boldsymbol{p}} = \boldsymbol{J}(\boldsymbol{q})\dot{\boldsymbol{q}}$ of the Jacobian matrix and rewriting $\boldsymbol{J}(\boldsymbol{q})$ as $\boldsymbol{J}$ for simplification, the Eq. (1) can be rewritten as:

$$\boldsymbol{J}^{-\mathrm{T}}\boldsymbol{B}(\boldsymbol{q})\boldsymbol{J}^{-1}\ddot{\boldsymbol{p}} + \boldsymbol{J}^{-\mathrm{T}}[\boldsymbol{C}(\boldsymbol{q},\dot{\boldsymbol{q}})\boldsymbol{J}^{-1} - \boldsymbol{B}(\boldsymbol{q})\boldsymbol{J}^{-1}\dot{\boldsymbol{J}}\boldsymbol{J}^{-1}]\dot{\boldsymbol{p}} + \boldsymbol{J}^{-\mathrm{T}}\mathbf{F}\boldsymbol{J}^{-1}\dot{\boldsymbol{p}} + \boldsymbol{J}^{-\mathrm{T}}\boldsymbol{g}(\boldsymbol{q}) = \boldsymbol{J}^{-\mathrm{T}}\boldsymbol{\tau}. \tag{2}$$

Renaming some equation terms, Eq. (2) can be resumed to:

$$\overline{\boldsymbol{B}}(\boldsymbol{q})\ddot{\boldsymbol{p}} + \overline{\boldsymbol{C}}(\boldsymbol{q},\dot{\boldsymbol{q}})\dot{\boldsymbol{p}} + \overline{\mathbf{F}}\dot{\boldsymbol{p}} + \overline{\boldsymbol{g}}(\boldsymbol{q}) = \gamma, \tag{3}$$

witch describes the dynamics of the robot manipulator in the operational space, with $\overline{\boldsymbol{B}}(\boldsymbol{q})$ being the symmetric inertia matrix, $\overline{\boldsymbol{C}}(\boldsymbol{q},\dot{\boldsymbol{q}})$ the Coriolis and centrifugal forces matrix and the frictional forces are related to the matrix $\overline{\mathbf{F}}$, all these matrices are in the operational space base. Still, $\overline{\boldsymbol{g}}(\boldsymbol{q})$ is the gravitational forces vector equivalent to the operational space and the joint torques vector $\boldsymbol{\tau}$ is related to the operational space by the forces vector γ.

For our tests, it was used a reduced mathematical model based on the first two joints of the robot, i.e., it was considered two degrees of freedom related to two rotational joints. Then, since the two rotational joint axes are parallels, the task space is reduced to a plane. Another consequence is that the gravitational forces vector become negligible, i.e., $\overline{\boldsymbol{g}}(\boldsymbol{q}) = \mathbf{0}$, this occurs because the gravitational force is parallel to the joints axes.

Below are detailed the matrices of the dynamic model that need to be computed to perform the control, as shown by Vargas “et al.” (2004).

Inertia matrix:

$$\boldsymbol{B}(\boldsymbol{q}) = \begin{bmatrix} \mathrm{a}_1 + 2(\mathrm{m}_2\mathrm{l}_1\mathrm{l}_{\mathrm{c}2} + (\mathrm{m}_3 + \mathrm{m}_4)\mathrm{l}_2\mathrm{l}_1)\cos(q_2) & \mathrm{a}_2 + (\mathrm{m}_2\mathrm{l}_1\mathrm{l}_{\mathrm{c}2} + (\mathrm{m}_3 + \mathrm{m}_4)\mathrm{l}_2\mathrm{l}_1)\cos(q_2) \\ \mathrm{a}_2 + (\mathrm{m}_2\mathrm{l}_1\mathrm{l}_{\mathrm{c}2} + (\mathrm{m}_3 + \mathrm{m}_4)\mathrm{l}_2\mathrm{l}_1)\cos(q_2) & \mathrm{a}_2 + \mathrm{j}_2\mathrm{k}_\mathrm{r}^2 \end{bmatrix},$$

$$\mathrm{a}_1 = \mathrm{a}_2 + \mathrm{i}_1 + (\mathrm{m}_2 + \mathrm{m}_3 + \mathrm{m}_4)\mathrm{l}_1^2 + \mathrm{m}_1\mathrm{l}_{\mathrm{c}1}^2 + \mathrm{j}_1\mathrm{k}_\mathrm{r}^2, \tag{4}$$

$$\mathrm{a}_2 = \mathrm{i}_2 + \mathrm{i}_3 + \mathrm{i}_4 + \mathrm{m}_2\mathrm{l}_{\mathrm{c}2}^2 + (\mathrm{m}_3 + \mathrm{m}_4)\mathrm{l}_2^2.$$

Coriolis and centrifugal forces matrix :

$$\boldsymbol{C}(\boldsymbol{q}, \dot{\boldsymbol{q}}) = \begin{bmatrix} -(\mathrm{m}_2\mathrm{l}_1\mathrm{l}_{\mathrm{c}2} + (\mathrm{m}_3 + \mathrm{m}_4)\mathrm{l}_2\mathrm{l}_1)\sin(q_2)\dot{q}_2 & -(\mathrm{m}_2\mathrm{l}_1\mathrm{l}_{\mathrm{c}2} + (\mathrm{m}_3 + \mathrm{m}_4)\mathrm{l}_2\mathrm{l}_1)\sin(q_2)(\dot{q}_1 + \dot{q}_2) \\ (\mathrm{m}_2\mathrm{l}_1\mathrm{l}_{\mathrm{c}2} + (\mathrm{m}_3 + \mathrm{m}_4)\mathrm{l}_2\mathrm{l}_1)\sin(q_2)\dot{q}_1 & 0 \end{bmatrix}. \tag{5}$$

Jacobian matrix:

$$\boldsymbol{J}(\boldsymbol{q}) = \begin{bmatrix} -\mathrm{l}_1\sin(q_1) - \mathrm{l}_2\sin(q_1 + q_2) & -\mathrm{l}_2\sin(q_1 + q_2) \\ \mathrm{l}_1\cos(q_1) + \mathrm{l}_2\cos(q_1 + q_2) & \mathrm{l}_2\cos(q_1 + q_2) \end{bmatrix}. \tag{6}$$

Frictional forces matrix:

$$\mathbf{F} = \begin{bmatrix} \mu_1 & 0 \\ 0 & \mu_2 \end{bmatrix}, \tag{7}$$

for simplicity, the friction matrix is considered to be composed only by dynamic friction coefficients. In Tab. 1 are detailed the parametric values that compose the dynamic model matrices.

Table 1. Inter robot manipulator parameters

Symbol	Description	Value
l_1 and l_2	Length of links 1 and 2	0.25 [m]
$\mathrm{l}_{\mathrm{c}1}$	Center of mass of link 1	0.118 [m]
$\mathrm{l}_{\mathrm{c}2}$	Center of mass of link 2	0.116 [m]
m_1	Mass of link 1	11.40 [kg]
m_2	Mass of link 2	19.50 [kg]
m_3	Mass of link 3	2.00 [kg]
m_4	Mass of link 4	1.50 [kg]
i_1	Moment of inertia of link 1	0.23 [kg.m^2]
i_2	Moment of inertia of link 2	0.16 [kg.m^2]
i_3	Moment of inertia of link 3	0.10 [kg.m^2]
i_4	Moment of inertia of the 4	0.10 [kg.m^2]
j_1 and j_2	Moment of inertia of the rotors	5.00×10^{-5} [kg.m^2]
μ_1	Viscous friction coeff. of joint 1	11.50 [Nms/rad]
μ_2	Viscous friction coeff. of joint 2	6.00 [Nms/rad]
k_r	Joints gear relation	100

3. PROPOSED CONTROLLER

The aim of the proposed controller is to perform tasks in the operational space based on a reduced algorithm, which means low computational load. This is achieved by inserting fuzzy logic in the control action. Such insertion has the function to replace the nonlinear terms of the matrix by means of fuzzy sets mapping.

The proposed control structure is based on a stiffness control strategy presented by Slotine and Li (1987), which uses the concept of an auxiliary error to achieve better rates of convergence to the tracking errors. The control action consists of a PD action, to obtain trajectory tracking due the modeling errors, and a model-based mapped term to compensate inertial forces.

Since the focus of this paper is to provide satisfactory results in tasks performed in the operational space allied to a low computational load, after some tests it was decided to neglect the terms derived from the Coriolis and centrifugal forces. The fundamental idea of the control action refers to a PD controller with addiction of a term that interacts with inertial forces. Moreover, the terms in the control action related to accelerations are based on the properties of the inertia matrix (positive definite), which can be considered as a gain matrix with positive variable values. Thus, the basic control action is given by:

$$\boldsymbol{\tau} = \boldsymbol{J}^{\mathrm{T}}[\mathrm{k_p}\tilde{\boldsymbol{p}} + \mathrm{k_d}\dot{\tilde{\boldsymbol{p}}} + \overline{\boldsymbol{B}}(\boldsymbol{q})\ddot{\boldsymbol{p}}_{\mathrm{d}}], \tag{8}$$

where $\tilde{\boldsymbol{p}} = \boldsymbol{p}_{\mathrm{d}} - \boldsymbol{p}$ is the end-effector position error vector, $\dot{\tilde{\boldsymbol{p}}} = \dot{\boldsymbol{p}}_{\mathrm{d}} - \dot{\boldsymbol{p}}$ is the end-effector velocity error vector, $\boldsymbol{p} = [x\ y]^{\mathrm{T}}$ is the end-effector position vector, $\boldsymbol{p}_{\mathrm{d}} = [x_d\ y_d]^{\mathrm{T}}$ is the desired position vector, $\dot{\boldsymbol{p}} = [\dot{x}\ \dot{y}]^{\mathrm{T}}$ is the end-effector velocity vector, $\dot{\boldsymbol{p}}_{\mathrm{d}} = [\dot{x}_d\ \dot{y}_d]^{\mathrm{T}}$ is the desired end-effector velocity vector and $\ddot{\boldsymbol{p}}_{\mathrm{d}} = [\ddot{x}_d\ \ddot{y}_d]^{\mathrm{T}}$ is the desired end-effector acceleration vector, all in the operational space. $\mathrm{k_p}$ and $\mathrm{k_d}$ are the proportional and derivative gains, respectively.

Compared to a simple PD controller, the control action shown in Eq. (8) presents a considerable reduction of the tracking errors provided by the addition of the term $\overline{\boldsymbol{B}}(\boldsymbol{q})\ddot{\boldsymbol{p}}_{\mathrm{d}}$. However, the convergence rate of the error can be increased by using the auxiliary error proposed by Slotine and Li (1987).

Thus, the controller action is modified to provide such increasing in the tracking:

$$\boldsymbol{\tau} = \boldsymbol{J}^{\mathrm{T}}[\mathrm{k_d}\boldsymbol{\sigma} + \overline{\boldsymbol{B}}(\boldsymbol{q})\ddot{\boldsymbol{p}}_{\mathrm{r}}], \tag{9}$$

where $\boldsymbol{\sigma} = \dot{\tilde{\boldsymbol{p}}} + \mathrm{k_p}\tilde{\boldsymbol{p}}$ is the filtered tracking error and $\dot{\boldsymbol{p}}_{\mathrm{r}} = \dot{\boldsymbol{p}}_{\mathrm{d}} + \mathrm{k_p}\tilde{\boldsymbol{p}}$ is the reference velocity based on the position error. In this stage the fuzzy logic is introduced to substitute the nonlinear functions by mapped functions.

This mapped functions are better understood by expanding the inertia matrix $\overline{\boldsymbol{B}}(\boldsymbol{q})$ and rewriting $\boldsymbol{B}(\boldsymbol{q})$ as $\boldsymbol{B}$ for simplicity, in the Eq. (9):

$$\boldsymbol{\tau} = \boldsymbol{J}^{\mathrm{T}}\mathrm{k_d}\boldsymbol{\sigma} + \boldsymbol{B}\boldsymbol{J}^{-1}\ddot{\boldsymbol{p}}_{\mathrm{r}}. \tag{10}$$

Then, the mapping is made over the transposed Jacobian $\boldsymbol{J}^{\mathrm{T}}$, which is represented by $\overline{\overline{\boldsymbol{J}^{\mathrm{T}}}}$, and over the matrix $\boldsymbol{B}\boldsymbol{J}^{-1}$, which is represented by $\overline{\overline{\boldsymbol{B}\boldsymbol{J}^{-1}}}$, yielding the following expression to the control law:

$$\boldsymbol{\tau} = \overline{\overline{\boldsymbol{J}^{\mathrm{T}}}}\mathrm{k_d}\boldsymbol{\sigma} + \overline{\overline{\boldsymbol{B}\boldsymbol{J}^{-1}}}\ddot{\boldsymbol{p}}_{\mathrm{r}}. \tag{11}$$

To complete the mathematical analysis on the controller, in the next section is described the stability analysis of the closed-loop system.

4. SYSTEM STABILITY ANALYSIS

Consider the mapped terms rewritten as follow:

$$\overline{\overline{\boldsymbol{B}\boldsymbol{J}^{-1}}} = \boldsymbol{B}\boldsymbol{J}^{-1}(\mathbf{I} + \boldsymbol{\Psi}_1), \tag{12}$$

$$\overline{\overline{\boldsymbol{J}^{\mathrm{T}}}} = \boldsymbol{J}^{\mathrm{T}}(\mathbf{I} + \boldsymbol{\Psi}_2), \tag{13}$$

where $\boldsymbol{\Psi}_1$ and $\boldsymbol{\Psi}_2$ are matrix that contain error functions related to the mapping and vary with the robot manipulator posture. Substituting Eq. (13) and Eq. (12) in Eq. (11), one can describe the closed loop dynamic system as:

$$(\mathbf{I} + \boldsymbol{\Psi}_1)\overline{\boldsymbol{B}}\dot{\boldsymbol{\sigma}} + (\mathbf{I} + \boldsymbol{\Psi}_2)\mathrm{k_d}\boldsymbol{\sigma} = (\overline{\boldsymbol{C}} + \overline{\mathbf{F}})\dot{\boldsymbol{p}} - \overline{\boldsymbol{B}}\boldsymbol{\Psi}_1\ddot{\boldsymbol{p}}. \tag{14}$$

From Eq. (14) it is possible to conclude that the system will be stable since achieved the conditions $\boldsymbol{\Psi}_1 > -\mathbf{I}$ and $\boldsymbol{\Psi}_2 > -\mathbf{I}$. This criteria can be verified in the mapping stage.

One can even note that is impossible to achieve null errors when the robot manipulator performs motion, because the perturbation is directly related to the velocity and acceleration of the end-effector in the operational space.

This remark can be better noted expanding the variable $\boldsymbol{\sigma}$ in such a way to rewrite Eq. (14) in terms of errors:

$$\overline{\boldsymbol{B}}(\ddot{\tilde{\boldsymbol{p}}} + \mathrm{k_p}\dot{\tilde{\boldsymbol{p}}}) + (\mathbf{I} + \boldsymbol{\Psi}_2)\mathrm{k_d}(\dot{\tilde{\boldsymbol{p}}} + \mathrm{k_p}\tilde{\boldsymbol{p}}) = -(\overline{\boldsymbol{C}} + \overline{\mathbf{F}})\dot{\tilde{\boldsymbol{p}}} + (\overline{\boldsymbol{C}} + \overline{\mathbf{F}})\dot{\boldsymbol{p}}_{\mathrm{d}} - \overline{\boldsymbol{B}}\boldsymbol{\Psi}_1\ddot{\boldsymbol{p}}_{\mathrm{d}}, \tag{15}$$

after some manipulation and substitution, Eq. (15) can be rewritten as,

$$\boldsymbol{\Gamma}_1\ddot{\tilde{\boldsymbol{p}}} + \boldsymbol{\Gamma}_2\dot{\tilde{\boldsymbol{p}}} + \boldsymbol{\Gamma}_3\tilde{\boldsymbol{p}} = (\overline{\boldsymbol{C}} + \overline{\mathbf{F}})\dot{\boldsymbol{p}}_{\mathrm{d}} - \overline{\boldsymbol{B}}\boldsymbol{\Psi}_1\ddot{\boldsymbol{p}}_{\mathrm{d}}, \tag{16}$$

where $\boldsymbol{\Gamma}_1 = \overline{\boldsymbol{B}}$, $\boldsymbol{\Gamma}_2 = (\mathbf{I} + \boldsymbol{\Psi}_1)\overline{\boldsymbol{B}}\mathrm{k_p} + (\mathbf{I} + \boldsymbol{\Psi}_2)\mathrm{k_d} + \overline{\boldsymbol{C}} + \overline{\mathbf{F}}$ and $\boldsymbol{\Gamma}_3 = (\mathbf{I} + \boldsymbol{\Psi}_2)\mathrm{k_d}\mathrm{k_p}$.

Thus, it is identified the direct relationship of the perturbation with the desired velocities, the term $(\overline{\boldsymbol{C}} + \overline{\mathbf{F}})\dot{\boldsymbol{p}}_{\mathrm{d}}$, and the desired acceleration, the term $\overline{\boldsymbol{B}}\boldsymbol{\Psi}_1\ddot{\boldsymbol{p}}_{\mathrm{d}}$. This way, with the absence of desired velocity and acceleration, i.e., in regulation cases, by the Eq. (16) we conclude that the error tends to zero when the time goes to infinite.

5. FUZZY MAPPING

In this section is described the mapping of the nonlinear matrices, $\boldsymbol{J}^{\mathrm{T}}$ and $\boldsymbol{BJ}^{-1}$, presented previously. The mapping area is restricted to the first quadrant of the robot manipulator workspace and delimited by a radius range of 295 mm to 495 mm, crosshatched in Fig. 3. The work plane is delimited at such a way only to avoid problems with singularity postures during the experiments.

In the Fig. 4 are depicted the graphical representation of each element of the nonlinear matrices $\boldsymbol{J}^{\mathrm{T}}$ and $\boldsymbol{BJ}^{-1}$, varying with the end-effector position in polar reference (angle and radius), concerning with the work plane.

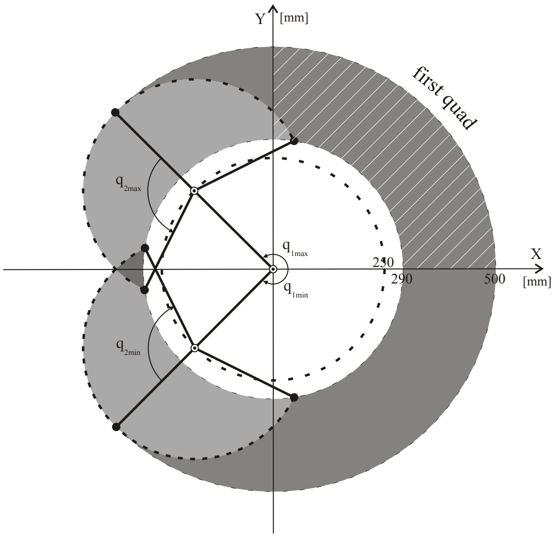

Figure 3. Work space of the SCARA robot

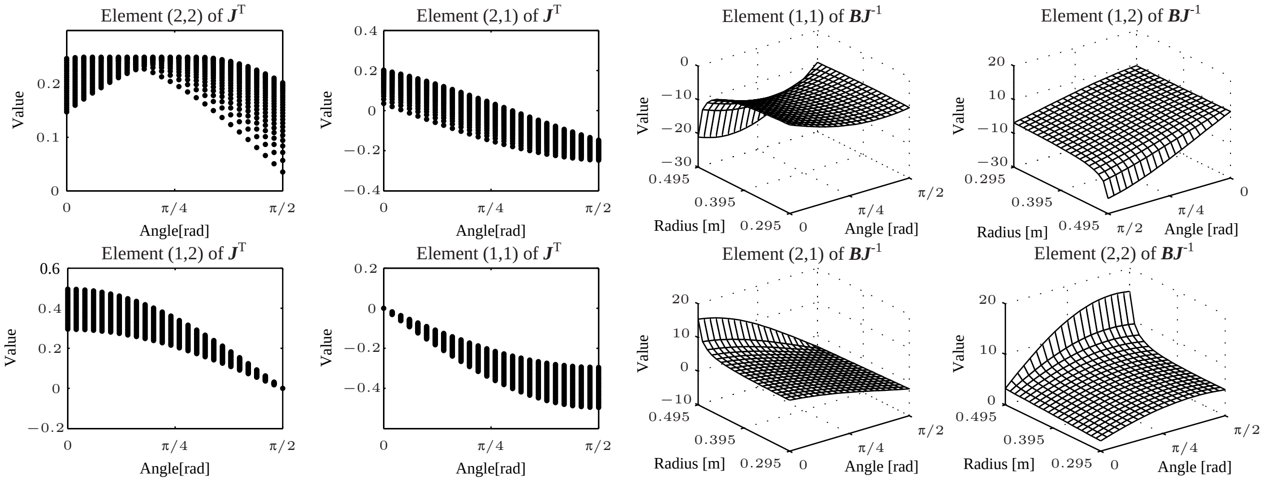

Figure 4. $\boldsymbol{J}^{\mathrm{T}}$ and $\boldsymbol{BJ}^{-1}$ and elements

The fuzzy set arrangement do not constitute of a trivial task and so this paper is not focused in the mapping optimization, but in its computational load and mapping accuracy (to fulfill the stability conditions). Future works will be driven to search for optimal mappings.

To the mapping task one has opted to use the Adaptive Neuro-Fuzzy Inference System Editor (ANFIS Editor), which is part of the fuzzy logic toolbox of the Matlab® software. This tool provides a back-propagation algorithm combined with a least square method to setup the fuzzy rules using a set of conjugate input/output pairs of the nonlinear matrices to be mapped.

The Sugeno inference method, the mapping process can use linear or constant output membership functions (MF), and the input MFs can be any equation that represents a statistical distribution. The selection of these MFs will influence directly in the accuracy and computational load of the controller.

Two arrangements of fuzzy mapping are tested in this work. The first one aims to a reduction of the mapping error using a generalized bell-shaped input MF, see Eq. (17), with linear output MF. The other arrangement aims to a reduction of the computational load in detriment of the mapping error using an triangular-shaped input MF, see Eq. (18), and a constant output MF.

$$gbellmf(z) = \frac{1}{1 + \left|\dfrac{z - \mathrm{c}}{\mathrm{a}}\right|^{2\mathrm{b}}}. \tag{17}$$

$$trimf(z) = max\left(min\left(\frac{z - \mathrm{a}}{\mathrm{b} - \mathrm{a}}, \frac{\mathrm{c} - z}{\mathrm{c} - \mathrm{b}}\right), 0\right). \tag{18}$$

In Eq. (17) and Eq. (18) the parameters a, b and c are obtained by the adaptive neuro-fuzzy system. The results for these mapping setups are shown in next section.

6. EXPERIMENTAL RESULTS

In this section the details of the experiment are described. To evaluate the performance of the fuzzy mapping approach on the terms $\boldsymbol{J}^{\mathrm{T}}$ and $\boldsymbol{BJ}^{-1}$, it was stipulated a desired trajectory in the work plane and tested the following three strategies: a basic PD control, a PD control with terms based on the model, described in Eq. (10), and the control described in Eq. (11), which has the model-based nonlinear terms mapped via fuzzy systems.

The desired trajectory, described in Eq. (19) and depicted in Fig. 5, is located in the first quadrant of the work plane, in such a way that one can use the mapping detailed in Section 5.

$$traj(t) = \begin{cases} f_1(t) = \begin{cases} x_{\mathrm{d}} = (0.39 + 0.08\sin(\pi t))\cos\left(0.039\pi t + \frac{\pi}{18}\right) \\ y_{\mathrm{d}} = (0.39 + 0.08\sin(\pi t))\sin\left(0.039\pi t + \frac{\pi}{18}\right) \end{cases} & t \leq 10\,\mathrm{s} \\ \\ f_2(t) = \begin{cases} x_{\mathrm{d}} = (0.39 + 0.08\sin(\pi(t-10)))\sin\left(0.039\pi(t-10) + \frac{\pi}{18}\right) \\ y_{\mathrm{d}} = (0.39 + 0.08\sin(\pi(t-10)))\cos\left(0.039\pi(t-10) + \frac{\pi}{18}\right) \end{cases} & 10\,\mathrm{s} < t \leq 20\,\mathrm{s} \end{cases}. \tag{19}$$

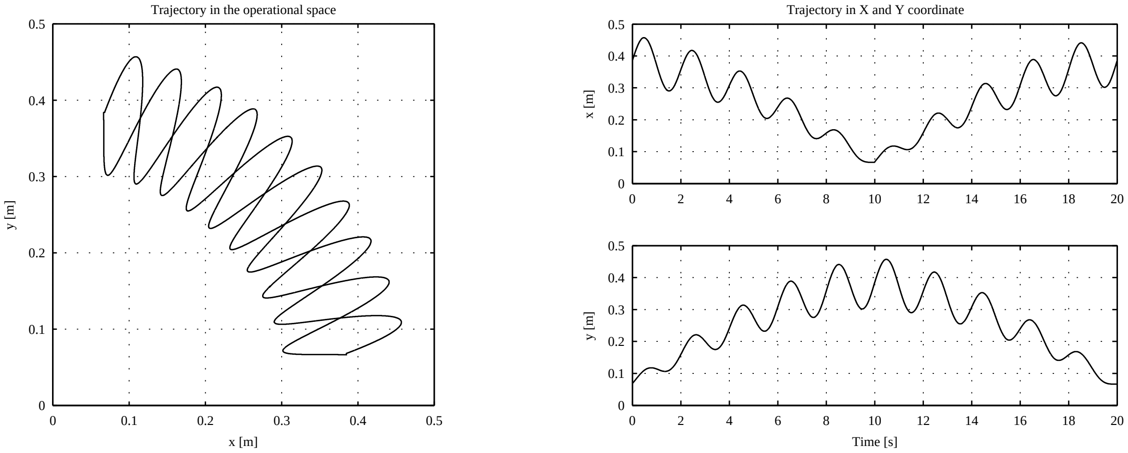

Figure 5. Task trajectory reference

Furthermore, to realize the effect of the nonlinear terms added in Eq. (10) as in Eq. (11), all PD actions in the three strategies have the same values, as detailed in Tab. 2.

Table 2. Equivalence of control actions

Controller	Gain value	Gain value	Equivalent proportional action	Equivalent derivative action
PD	$\mathrm{k_p} = 20000$	$\mathrm{k_d} = 200$	$\mathrm{k_p} = 20000$	$\mathrm{k_d} = 200$
PD+MBT[1]	$\mathrm{k_p} = 100$	$\mathrm{k_d} = 200$	$\mathrm{k_p k_d} = 20000$	$\mathrm{k_d} = 200$
PD+FMT[2]	$\mathrm{k_p} = 100$	$\mathrm{k_d} = 200$	$\mathrm{k_p k_d} = 20000$	$\mathrm{k_d} = 200$

[1] Model Based Term.

[2] Fuzzy Mapped Term.

It is important to mention that the robot has harmonic drives as transmission system device, therewith the friction effects are significantly witnessed. Thus, to improve the quality of the controller a simple friction compensation could be inserted in parallel to the PD strategy. However for the tests were only used the controllers specified up to now, i.e., friction compensation is not employed.

6.1. Control Strategies Performance

Based on the experiments, in Fig. 6 one can observe that the PD+MBT (Model Based Term) controller presents a considerable reduction of the tracking errors, when compared with the PD controller. From the information depicted in the graphic of the task performance, see Fig. 7 (left), one can verify that the PD controller shows a quadratic error of 6.01×10^{-3} m with variance of 15.05×10^{-6} and the PD+MBT controller shows an error of 3.77×10^{-3} m with variance of 3.48×10^{-6}. These data came to realize the improve of quality on the PD+MBT controller over the only PD one.

Another important feature to be mentioned is the difference between control actions, as shown in Fig. 7 (right). The magnitude of the control action is reduced once the levels of tracking are increased due to the model-based terms added in the control law.

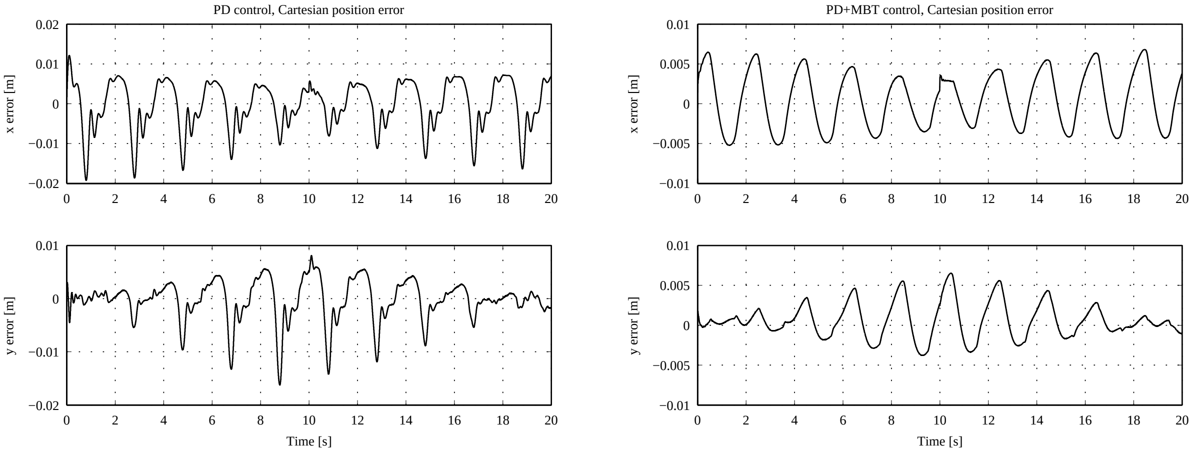

Figure 6. Trajectory tracking errors

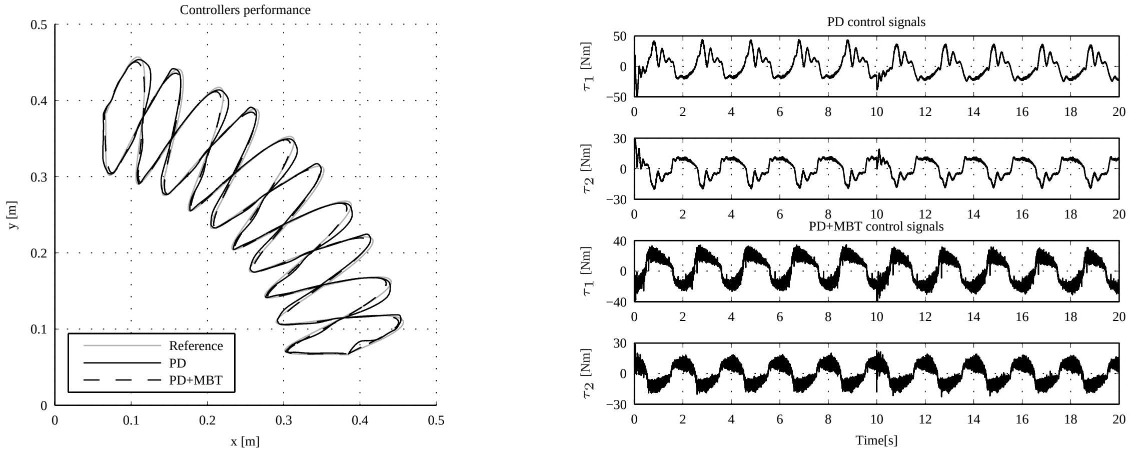

Figure 7. Control position performance and control signals

6.2. Reducing the computational load

As presented in Section 5, to reduce the computational load, a fuzzy map over the nonlinear model matrices is proposed. In the Tab. 3 one can see the setup parameters used in the mapping process and the calculated error for each element of the matrix $\boldsymbol{J}^{\mathrm{T}}$, i.e., input variables, number of input MFs for each element, sort of each input and output MF and maximum errors obtained in the mapping.

The setup information is only presented for further reproduction. The error is the head information obtained and serves to evaluate the mapping process over the system stability, as presented in Section 4.

Table 3. $\boldsymbol{J}^{\mathrm{T}}$ mapping configuration parameters and error

Setup parameters					Calculated error
Element	Input vars	Number of MFs	Input MF type	Output MF type	
$\overline{\overline{\boldsymbol{J}}}^{\mathrm{T}}_{11}$	angle	3	trimf	continuous	0.040
$\overline{\overline{\boldsymbol{J}}}^{\mathrm{T}}_{12}$	angle	3	trimf	continuous	0.040
$\overline{\overline{\boldsymbol{J}}}^{\mathrm{T}}_{21}$	angle	3	trimf	continuous	0.024
$\overline{\overline{\boldsymbol{J}}}^{\mathrm{T}}_{22}$	angle	3	trimf	continuous	0.046

To visually compare the mapped functions, one can see the original function elements of the matrix $\boldsymbol{J}^{\mathrm{T}}$ at Fig. 4 (left) and the mapped elements at Fig. 8.

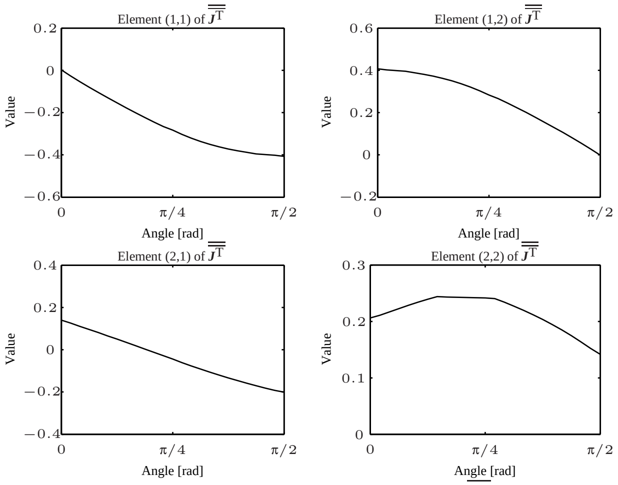

Figure 8. Mapped elements of $\overline{\overline{\boldsymbol{J}}}^{\mathrm{T}}$

For the matrix $\boldsymbol{J}^{\mathrm{T}}$ one can find that the mapping process, utilizing triangular functions and at most three input MFs, presents sufficient low computational load at high mapping performance (low error). So the mapping of this matrix stated no problem since it is a matrix with nonlinearities subordinated to only one input variable.

Already with respect to the matrix $\boldsymbol{BJ}^{-1}$, it has three dimensional elements and its computational time become a problem to be solved. As reported in Section 5, two kinds of mapping are made and compared for this matrix, one utilizing an accurate mapping and other valuing the low computational load. So the mapping process focuses in the trade off accuracy/load.

Table 4 depict the setup parameters and the calculated errors obtained for the matrix $\boldsymbol{BJ}^{-1}$ utilizing the accurate mapping process, i.e., utilizing the input function $gbellmf(z)$ (Eq. (17)) and a linear output MF. This results compared to the results shown in Tab. 5, that shows the mapping setup parameters and errors for the low cost mapping process, shows a huge mapping accuracy for the first mapping process. Nevertheless, in practical tests, the high accuracy of the first method presents higher computational load compared to the second one, and the performance results do not show sufficient differences. The two process of mapping present so similar performance results that the accurate one proved to be not a good choice.

Table 4. $\boldsymbol{BJ}^{-1}$ accurate mapping configuration parameters and error

Setup parameters					Calculated error
Element	Input vars	Number of MFs	Input MF type	Output MF type	
$\overline{\overline{\boldsymbol{BJ}}}^{-1}_{11}$	angle and radius	[3 3]	gbellmf	linear	0.098
$\overline{\overline{\boldsymbol{BJ}}}^{-1}_{12}$	angle and radius	[3 3]	gbellmf	linear	0.070
$\overline{\overline{\boldsymbol{BJ}}}^{-1}_{21}$	angle and radius	[3 3]	gbellmf	linear	0.050
$\overline{\overline{\boldsymbol{BJ}}}^{-1}_{22}$	angle and radius	[3 3]	gbellmf	linear	0.066

In Fig. 9 one can see the visual representation of the two mapping process, the accurate (left) and the low cost (right) one, this two mapping, can be compared to the original matrix at Fig. 4 (right).

Table 5. $\boldsymbol{BJ}^{-1}$ low cost mapping configuration parameters and error

Setup parameters					Calculated error
Element	Input vars	Number of MFs	Input MF type	Output MF type	
$\overline{\overline{\overline{\boldsymbol{BJ}}}}^{-1}_{11}$	angle and radius	[3 2]	trimf	continuous	0.563
$\overline{\overline{\overline{\boldsymbol{BJ}}}}^{-1}_{12}$	angle and radius	[2 2]	trimf	continuous	0.575
$\overline{\overline{\overline{\boldsymbol{BJ}}}}^{-1}_{21}$	angle and radius	[2 2]	trimf	continuous	0.424
$\overline{\overline{\overline{\boldsymbol{BJ}}}}^{-1}_{22}$	angle and radius	[2 2]	trimf	continuous	0.646

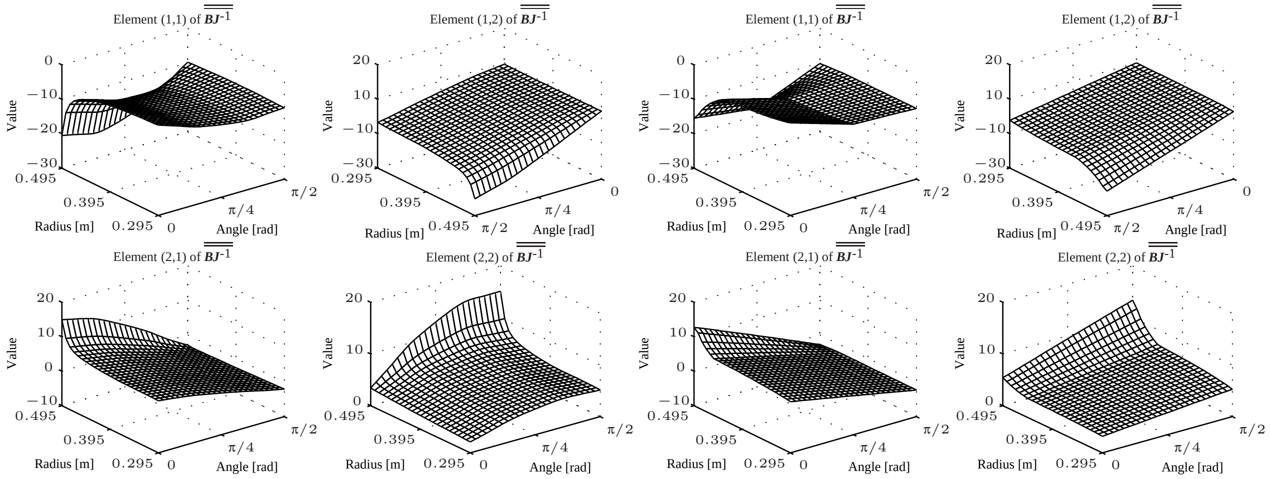

Figure 9. Mapped elements of $\overline{\overline{\overline{\boldsymbol{BJ}}}}^{-1}$

As a last result, the performance of the mapped controller is show in the Fig. 10. Compared to the reference trajectory, the calculated quadratic error is 3.85×10^{-3} and its variance is 3.40×10^{-6}. This validate the mapping process as a good choice to maintain the performance of the controller with a lower computational load. The load reduction is explained by the reduction in the order of the nonlinear matrices, now represented by the mapped ones, and the eminent elimination of the nonlinear terms and some matrix operations.

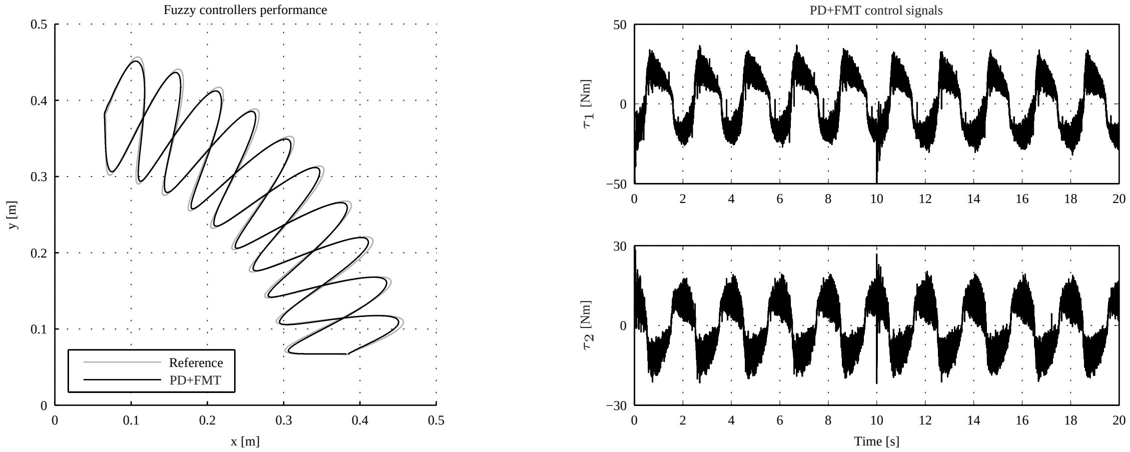

Figure 10. Performance of the PD+FMT controllers

7. CONCLUSION

In this paper is proposed a control action for robot manipulators, based on the stiffness control strategy presented by Slotine and Li (1987), where the task and the control are performed in the operational space. Since this strategy is basically a PD action with an addition of a model based term (PD+MBT), it provides a considerable improvement in the results (lower levels of error) at the expense of a computational load larger than a simple PD.

To circumvent the computational load problem, a mapping of the nonlinear terms of the controller (PD+FMT) is proposed and experimentally tested over a SCARA configuration robot. One concludes that the fuzzy mapping with high accuracy can lead to greater computational load, not being a good choice for the task control. However, if the mapping process is made by reducing the accuracy, this fuzzy approach can present satisfactory results, without considerable loss of tracking quality, with reduced computational load.

8. REFERENCES

Mamdani, E.H., 1974. "Application of fuzzy algorithms for control of simple dynamic plant". Proceedings of the Institution of Electrical Engineers UK, Vol. 121, No. 12, pp. 1585–1588. <doi:10.1049/piee.1974.0328>.

Sciavicco, L. and Siciliano, B., 2000. "Modelling and control of robot manipulators". Springer. <ISBN 1852332212>.

Siciliano, B. and Khatib, O., 2008. "Springer handbook of robotics". Springer. <ISBN 978-3-540-30301-5>.

Slotine, J.J.E. and Li, W., 1987. "On the adaptative control of robot manipulators". International Journal of Robotics Research, Vol. 6, pp. 49–59. <doi:10.1177/027836498700600303>.

Takagi, T. and Sugeno, M., 1985. "Fuzzy identification of systems and its applications to modeling and control". IEEE Transactions on Systems, Man, and Cybernetics, Vol. 15, No. 1, pp. 116–132. <URL http://takagiken.com/takagi-sugeno-modeling.pdf>.

Tanaka, K. and Wang, H.O., 2002. "Fuzzy control systems design and analisis: a linear matrix inequality approach". John Wiley & Sons, Inc. <doi:10.1002/0471224596>.

Vargas, F., De Pieri, E. and Castelan, E., 2004. "Identification and friction compensation for an industrial robot using two degrees of freedom controllers". Proceedings of the Control, Automation, Robotics and Vision Conference, Vol. 2, pp. 1146–1151. <doi:10.1109/ICARCV.2004.1469006>.

Zadeh, L.A., 1973. "Outline of a new approach to the analysis of complex systems and decision processes". IEEE Transactions on Systems, Man and Cybernetics, Vol. SMC-3, No. 1, pp. 28–44. <doi:10.1109/TSMC.1973.5408575>.

Zhang, H. and Liu, D., 2006. "Fuzzy modeling and fuzzy control". Birkhäuser. <doi:10.1007/978-0-8176-4539-7>.

9. RESPONSIBILITY NOTICE

The authors are the only responsible for the printed material included in this paper.